White Paper #XXXVII (formerly #XXXIX)

Why the Last Century's Quantum Mechanics (QM) is Irrelevant in a Duplex, Reciprocal Subspace, Reference Frame for Our Cognitive World

By

William A Tiller, Ph.D. and Walter E. Dibble, Jr., Ph.D.

Introduction

Nature is always richer in untapped possibilities than we think it is. We must always keep planting the new "seed corn" of fundamental research so that we might reveal new levels of nature's expression, which might look like new levels of "magic" as interpreted by the old paradigm. This is because the structural foundations of the old paradigm are **incapable** of explaining the new data. However, all of this **new** data can appear lawful and understandable via a **new** conceptual framework for a **new** paradigm. This, in turn, lays the foundation for abundant new applications that utilize this new knowledge. This provides new opportunities to test ourselves, to become **more** than we were and to show others how they can do likewise.

It is time to help the **quantum mechanical (QM) paradigm** to expand significantly beyond what it presently is! As presently formulated mathematically, quantum mechanics is a very precise theory whose reference frame (RF) of mathematics is a four-dimensional spacetime-only RF within the classical electric particle velocity limits from zero to the velocity of electromagnetic (EM) light, c, in physical vacuum, and involving the four fundamental forces discovered by establishment science to date of (1) gravity (2) Maxwellian electromagnetism (3) the long-range nuclear force and (4) the short-range nuclear force. This theory has been remarkably successful for particle physics, small atoms, molecules and photons. However, many of the outcomes from today's experiments are requiring weirder and weirder explanations. This is a clear sign that the present conceptual framework of quantum mechanics has reached the limits of its useful modeling capabilities.

Julian Schwinger,[(1)] along with Feinman and Tomanaga, shared the Nobel Prize for their discovery and mathematical development of quantum electrodynamics (QED). Schwinger had a Ph.D. student Paul Werbos, who made the very prophetic points[(2)] that (1) all forms of quantum electrodynamics : Copenhagen, Bohmian, Schwinger-type or Werbos-type yield the same kind of predictions and **none of them** can explain something like "remote viewing" (I assert that his statement applies to **any psychoenergetic phenomenon)**, and (2) he tells us that the world has spent billions of dollars to use quantum electrodynamics in the military to see things very far away and it has completely failed to do

so. The point, here, is that our present formulation of quantum mechanics, great as it is, is totally inadequate to encompass the inclusion of psychoenergetic phenomena into our scientific worldview. Thus, it is time to formulate a **larger** perspective or scientific reference frame for viewing nature that **both** accounts for all of the old data and also provides the possibility of quantitatively accounting for this new psychoenergetic data in an internally self-consistent way.

Harrison[3] has shown that **all** the applications of the last century's QM can be properly calculated provided that one assumes **the simultaneous existence in nature of both a particle and a wave expression for any physical substance!**

A serious scientific problem, as this author sees it, is that, **cognitively,** none of us has ever seen continuous waves like those drawn in science textbooks. The actual waves that most humans see or hear in today's world are all **modulations of particle** densities or modulations of **particle** fluxes. In any event, it is the oscillatory, time-dependent, bunching of particles to create the **envelope shapes** that we name as waves cognitively.

Because of this, the founding fathers of QM **should have** taken the **large step** of creating and using **a different reference frame** for the **waves** than for the **particles,** however, they did not, they tried to squeeze it all into a spacetime-only reference frame (RF) and thus ended up in perpetual weirdness for QM physics!

Via this author's[4,5] and his colleague's[4] intellectual creation of a duplex RF consisting of two, reciprocal, four-dimensional subspaces, one of which is spacetime, plus a coupler substance[6], allows a substance's particle-nature to function in spacetime (D-space), its wave-nature to function in Reciprocal space (R-space) and what has been labeled "deltrons" to function as the coupler substance. Thus, in this particular RF, particles **and** waves **simultaneously** function in an expanded physical reality!

What this actually means is that, since D-space is treated as the coarse electric, physical space, (where both, most of the space **between** the fundamental particles making up the coarse electric atoms and molecules and what we call "outer-space' (where a negligible electric atom/molecule density exists)), can be considered as a **non-dispersive** physical vacuum medium for electric substance (current experimental data shows that coarse EM-waves of all frequencies travel through physical vacuum **without** diminution of velocity due to interactive scattering). Thus, the very simple relationship of $\mathbf{v = \lambda f}$ (v = velocity, λ = wavelength and f = frequency) holds for all electromagnetic waves and therefore Eisberg's simple analysis[7] also holds. This unequivocally leads to the result given in Figure 1a that shows:

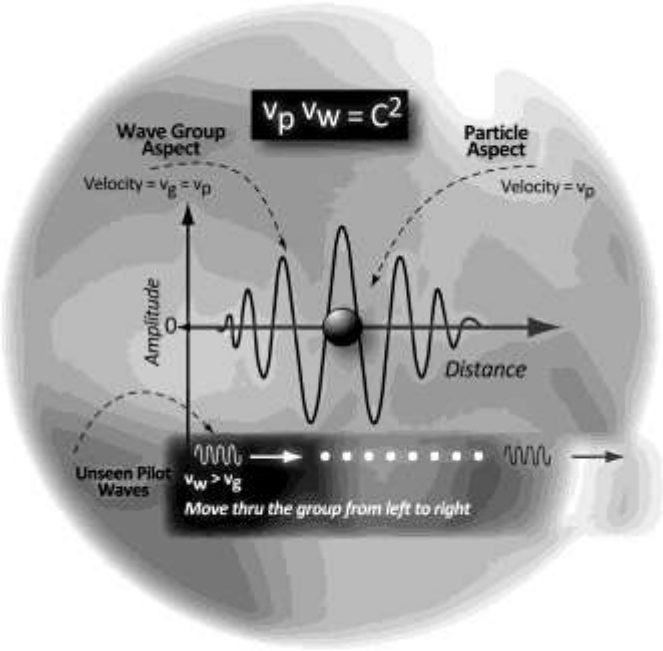

Figure 1a. Schematic of true pilot waves.

1. The electric particle velocity, v_p, equals the group wave velocity, v_g, illustrated in Figure 1b

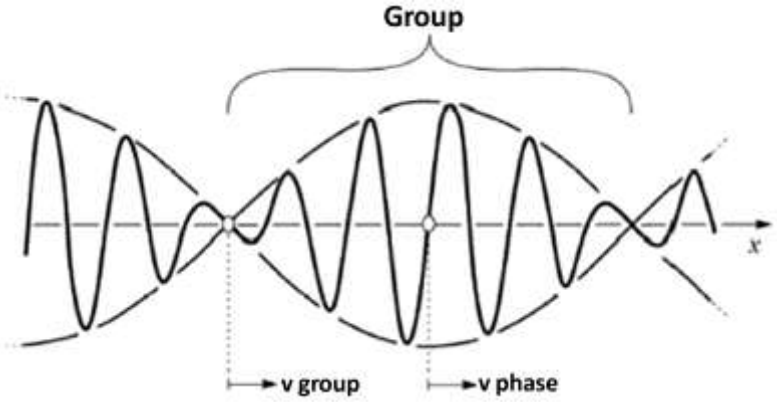

Figure 1b. Example of a group of waves moving along the x-direction. The entire group of wavelets propagates with group velocity v_{group}. Individual wavelets propagate with phase velocity v_{phase}.

2. Both of these travel at v less than the velocity of light in physical vacuum, v = c, and
3. DeBroglie's pilot wave, v_w, is calculated to travel at velocities faster than v_p less than c which means that v_w is superluminal and thus both invisible to most human's eyesight and to all of our

orthodox science instruments from a D-space mathematical perspective. This means that any R-space substance and R-space natural phenomena in today's world must be treated as mathematically imaginary.

Thus, from this interactive duplex space perspective, at least at this point in time, any single point in that space has a mathematically dual character which, in a two-dimensional Euclidian Geometry, for a D-space-only RF looks like Figure 2. The algebra needed for working with this kind of system is the algebra of complex variables[8]. As one might guess, expanding this Argand diagram concept of Figure 2 to this particular duplex space concept leads to a new way of looking at our world. Using the D-space-only Argand diagram example, the standard complex variable approach, is to define a complex number, z, as

$$z = x + iy \; or \; z = x + yi \quad ; \quad i = \sqrt{-1} \qquad (1a)$$

where i is called the imaginary unit.

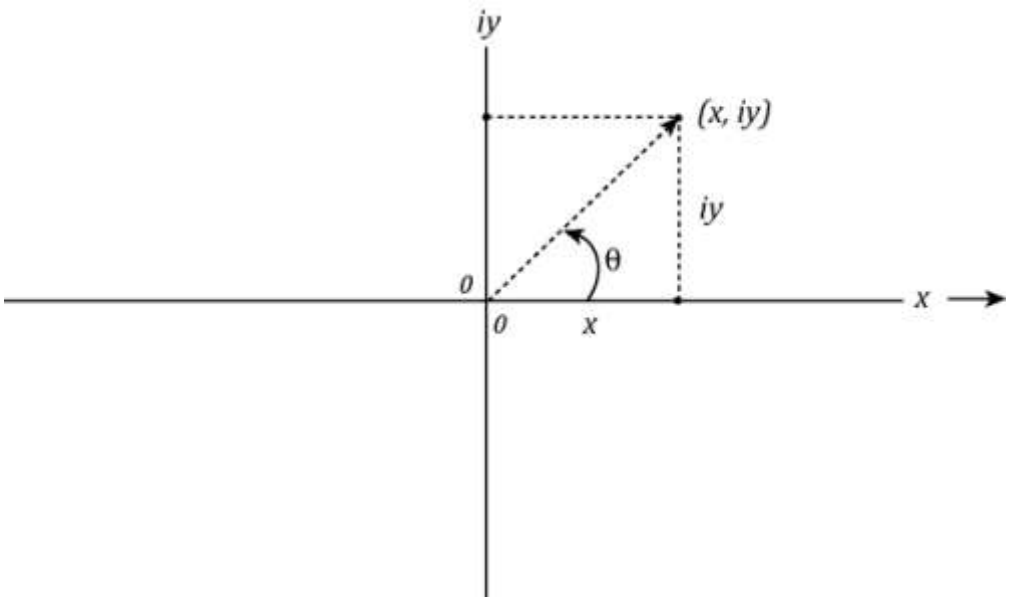

Figure 2. Illustration of a point at position, (x,iy), in a two-dimensional Euclidian, mathematically complex space with real abscissa and imaginary ordinate (a complex number z can be defined as z = x + iy or x + yi – this is called an Argand diagram)[8].

At this point, the important thing for us to recognize here is that the point, z = x +iy, can be treated as a vector with amplitude, $|x + iy|$, and phase angle, θ, relative to the x-axis. Because the symbol, | |, means the absolute value, the amplitude of the vector is always positive. Likewise a line connecting any two points in an Argand diagram is also a vector. If x and y in Figure 2 are real, the nonnegative real number, $\sqrt{x^2 + y^2}$, is called the **absolute value** or **modulus** of the complex number z. thus, by definition,

$$|z| = |x + iy| = \sqrt{x^2 + y^2} \quad . \qquad (1b)$$

Further, any quality, like a particular substance property or energy can be represented by a point in the Argand diagram with the vector magnitude being totally defined by

$$z = |z| \exp(i\theta) = |z|(cos\theta + isin\theta). \quad (1c)$$

Thus, as θ increases from 0^o to 360^o the exponential term, $e^{i\theta}$, moves from the first quadrant, (positive valued, so z is positive) to the second and third quadrants (negative valued so z is negative) to the fourth quadrant (again positive valued so z is positive). In this type of formal mathematical Argand diagram representation, we can begin to understand what Dirac's "**negative energy sea**" means for the source of electric matter and antimatter particles in our D-space world[9]. Here, in our simplest, one-dimensional, duplex, reciprocal subspaces world of a subluminal D-space and a superluminal R-space with coupler (from a D-space cognitive perception), we can explain many phenomena that have been misunderstood in the past. Let us look at some examples, to illustrate the concepts involved via the Argand diagram metaphor.

A. The Placebo Effect[10]

This example has been meaningfully discussed in Reference 10 so that only a brief summary will be given here.

Our experimental work of the 1997-2000 period[4] showed, unequivocally, that human consciousness, in the form of specific human intentions, can robustly alter the properties of materials as illustrated in Figure 3.

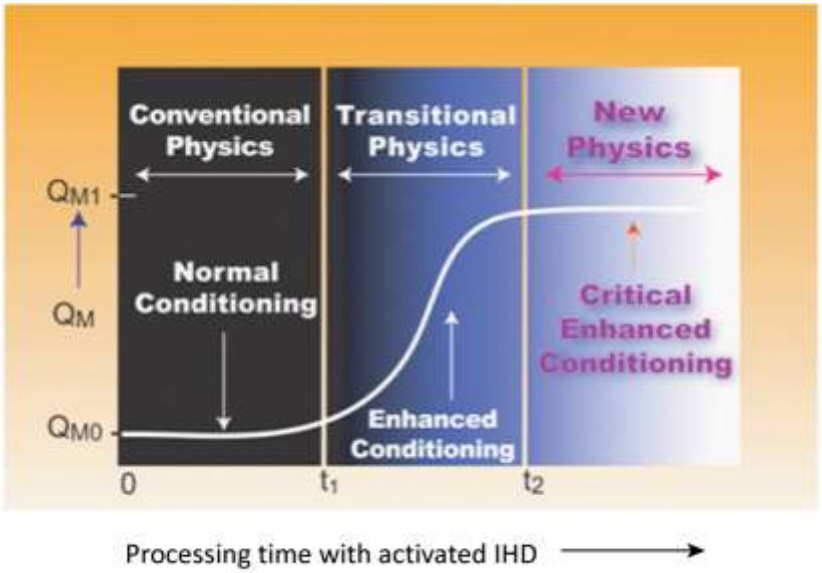

Figure 3. For any typical physical measurement, Q, the qualitative magnitude change, Q_M, is plotted versus the degree of locale conditioning produced by continued IHD use.

Let us call, Q, the material property to be explored and, $Q_M(t)$, the experimentally measured magnitude of that particular property as a function of time, t, during the experiment. In a zeroth-order mathematical approximation, we found that

$$Q_M(t) = Q_e + \alpha_{eff}(t) Q_m \, . \qquad (2)$$

Here, Q_e is our normal D-space contribution, Q_m is its R-space counterpart (superluminal) and α_{eff} is the coupling coefficient joining these two contributions in our duplex subspaces world. Thus, our current working hypothesis is that what we call **physical reality** consists of two unique categories of substance (subluminal and superluminal) in the same physical space. However, only one, Q_e, is accessible to our present-day orthodox (subluminal) measurement instruments when α_{eff} is zero.

The R-space level of physical reality (superluminal) is **invisible** to traditional physical, chemical, medical instruments when the system is in the **uncoupled state** ($\alpha_{eff} = 0$), but is accessible to these same instruments when the system is in the coupled state ($\alpha_{eff} > 0$). This second level (R-space) is the level of reality being largely manifested via human psychophysiology and is the experimental domain being pursued by CAM (complementary & alternative medicine).

These two, unique levels of reality can be partially coupled via (a) a simple electrical intention-host device (IHD) that (i) increases the magnitude of α_{eff} and (ii) directs it towards a specific purpose or (b) a significant biofield subtle energy emission from a human.

One of this author's working hypotheses is that Figure 4 provides a simple picture of the five key factors involved in any vector-system's interactive relationship. In this regard, it is useful for us to have a mental picture as to how we operate in life with respect to one another. Usually, all five components of Figure 4 may be intimately involved in the system's interactions. Now, let us look at the classical medical experiment with a placebo such as illustrated in Figure 4 (neglecting the "unseen" and higher Gauge symmetry states as in Figure 5).

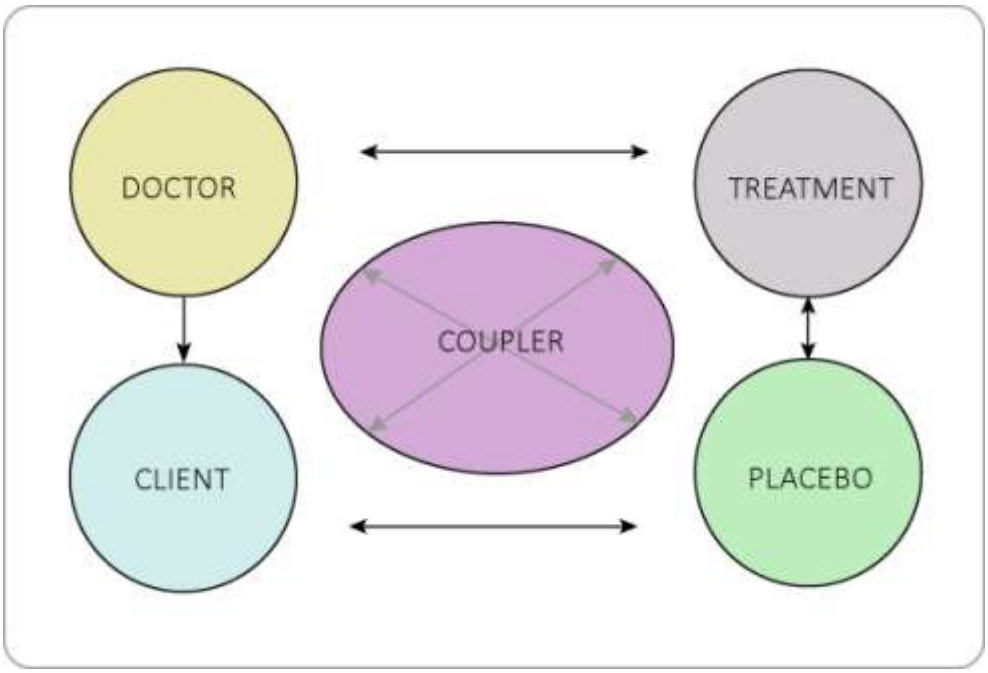

Figure 4. Illustration of a typical medical vector-system experiment.

My interest in this phenomenon of Nature began on reading a short 1999 paper by Enserink[11] who noted how greatly the placebo effect's magnitude in double-blind pharmacological studies had grown in the previous 15 years. He pointed out that, "when companies started testing drugs for obsessive – compulsive disorder (OCD) back in the mid-1980's, the placebo response rate in this old testing was almost zero". Thus, the normal experimental assumption that the placebo in the experimental protocol was an inert participant was a good approximation to the truth at that time.

However, as time passed, the placebo response rates began to creep upwards to a point in 1999 where they were 70% to 80% of the treatment response rates and one could reasonably conclude that some clinical trials failed because of high placebo response rates. How is this possible if the placebo behaves in the overall experiment as an inert object? Let us look into that, because according to Equation 2, if something is happening in Nature to cause α_{eff} to slowly increase with time, but in an accelerating fashion, then the connectivity between things would likewise increase in an accelerating fashion and the second term on the right of Equation 2 could be of negligible size in the mid-1980's and of a significant portion of Q_M in 2000.

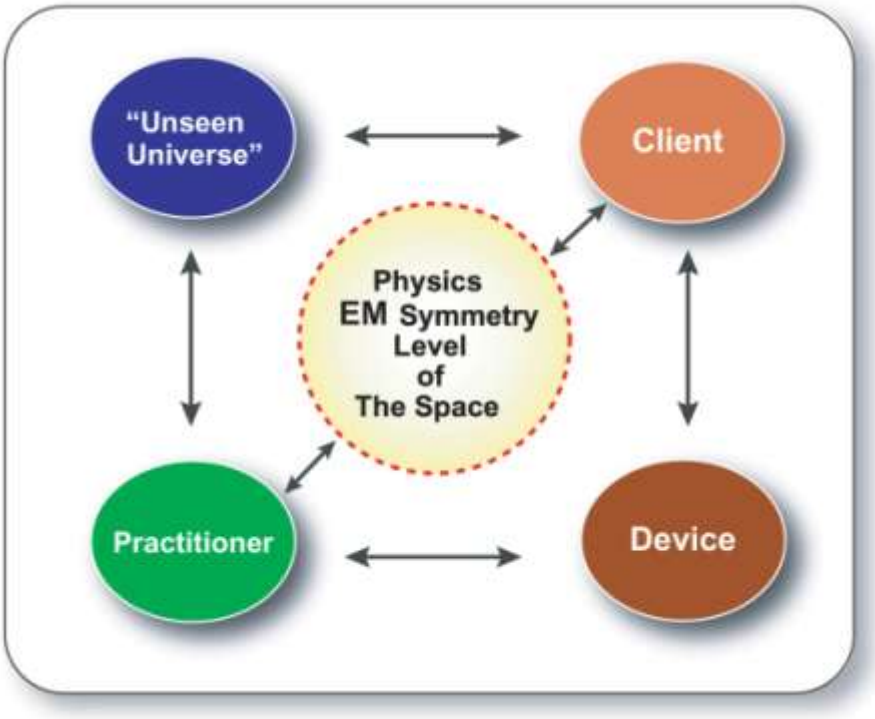

Figure 5. The simplest possible general communication system between practitioner and client in CAM.

In Appendix I, the magnetic information wave aspect of the system represented by Figure 5 has been worked out and one can readily see that a macroscopic information entanglement between all of the designated subsystems of the overall system can occur and further, that this piece of physics is the origin of the placebo effect. The relevant aspects of physics are the following:

(1) In R-space, each subsystem must be represented as a vector with both amplitude, $R(\underline{k})$, and phase angle, $\theta(\underline{k})$, where each is a function of the position coordinate, $\underline{k}$, in R-space,
(2) The entire system's vector, $R_S(\underline{k})\exp[i\theta_S(\underline{k})]$, is given by the vector sum (head to tail addition) of all the subsystem vectors converted first to common units, where exp = the exponential function and i = the imaginary number $(-1)^{1/2}$ (or $i^2 = -1$).
(3) Experimentally, one measures the system intensity I_S which is given by R_S^2 and which involves $R_S\ exp(-i\theta_S)$, multiplied by its complex conjugate, $R_S^*\ exp(+i\theta_S)$, which eliminates the 'imaginary' part to give a mathematically 'real' quantity.
(4) I_S is given by two groups of terms, (a) the sum of the squares of each vector amplitude and (b) the sum of pairs of different vector amplitudes multiplied by the cosine of the phase angle differences between these pairs and
(5) the total information entanglement for the Figure 5 system is given from 4b above.

Now, let us consider a typical clinical trial involving the subsystems (i) doctors, D, (ii) treatment, T, (iii) placebo, P, and (iv) subjects, s. For such a system event written in the Equation 1 format using the suffices of these subsystems, the placebo-effect magnitude will be given from Appendix 1 by

$$Q_{MP} = Q_{eP} + \alpha_{eff} \int_{\underline{k}} \left[R_P^2 + 2 \left\{ \begin{array}{l} R_P R_D \cos\left(\theta_P - \theta_D\right) + \\ R_P R_T \cos\left(\theta_P - \theta_T\right) + \\ R_P \bar{R}_S \cos\left(\theta_P - \bar{\theta}_S\right) \end{array} \right\} \right] d\underline{k} \; . \qquad (3)$$

B. The Electrodermal Voll Dermatron Diagnostic Device[(10)]

The relevant figure here is Figure 5, where the device (a Voll Dermatron or equivalent) acts much like the **placebo** in the Example A experiment. Reference 10 provides a description and discussion of the electrodermal measurement process while the Voll Dermatron was a popular commercial device for such a diagnostic investigation instrument for testing the state of a human's health in the 1970-1980s. With such a system, a sensitive practitioner was able to make remarkably sensitive predictions of the particular human's health state and also predictions of viable remedies that "seem to produce and sustain a condition of excellent health for that human!"

However, the FDA could not understand how such a device could possibly produce **any** efficacious results. Taking the device **out of the system** and measuring its properties, they found it to be very predictable to standard electrical engineering behavior. Thus, the FDA **convinced** themselves that there could be no possibility of its beneficial use to the practitioner except **as a fraud**. They raided such practitioners, confiscated all such devices and shut such practitioners down – wrongly (based upon our present understanding of a system of vectors as the proper mathematical perspective in today's world,

$$Q_{MD} = Q_{eD} + \alpha_{eff} \int_{\underline{k}} \left[R_D^2 + 2 \left\{ \begin{array}{l} R_{DP} \cos\left(\theta_D - \theta_P\right) + \\ R_{DC} \cos\left(\theta_D - \theta_C\right) + \\ R_{DU} \cos\left(\theta_D - \theta_U\right) \end{array} \right\} \right] d\underline{k} \; . \qquad (4)$$

C. A Preferred Alternate Explanation for Young's Double-Slit Experimental Result

In today's world, the classical Young's Double Slit experiment:

A. Can be carried out with single photons, one at a time, projected towards a screen but with an intermediate device placed in its path. This device has the capability of opening either one or two parallel and vertically oriented slits, separated by a constant distance, through which the photon may

pass on its travel to the screen. The operator has the ability to open either (1) the left slit only, (2) the right slit only or (3) both slits. The experimental observations for these three options are as follows:

(a) For only a single slit open, either left or right, the screen shows a single band of light behind the **open** slit (that has grown in intensity as the number of photons increases).
(b) For both slits open, **an interference pattern** of the slits, in the screen area behind the slits of photon collisions between the two slits is observed.

These observations have been interpreted as unequivocal evidence for a photon's dual behaviors as **both** a particle **and** a wave. This became a key cornerstone of quantum mechanics (QM).

In his forthcoming book[12], Omura properly points out that "slowing down the rate of photon-firing to one quantum at a time so that no two photons can interact with each other to create an in-flight interaction (and thus an interference pattern á la Young). So how can such a photon interference pattern be observed because only one particle was present in the experimental apparatus at any given time"?

B. To answer the foregoing question, let us shift our attention to this author's research results on psychoenergetic science[4-6] and D-space/deltron/R-space interactions. From these references one finds that a more appropriate reference frame (RF) than spacetime-only for the founding fathers of QM to have used, before embarking on the QM adventure, would have been a biconformal or duplex RF comprised of two, 4-dimensional, reciprocal subspaces, one of which is spacetime. The reciprocal symmetry of such a subspace pair has the unique advantage that a material property in one subspace has an equilibrium thermodynamic conjugate property in the reciprocal subspace (R-Space) given by a deltron-coupler-modified, Fourier Transform pair relationship[13]. In References 4 and 5, a variety of one-dimensional to three-dimensional spacetime objects have been utilized for mathematical calculations of the reciprocal-space conjugates for the special case of complete coupling.

The one-dimensional example is shown in Figures 6(a) and 6(b).

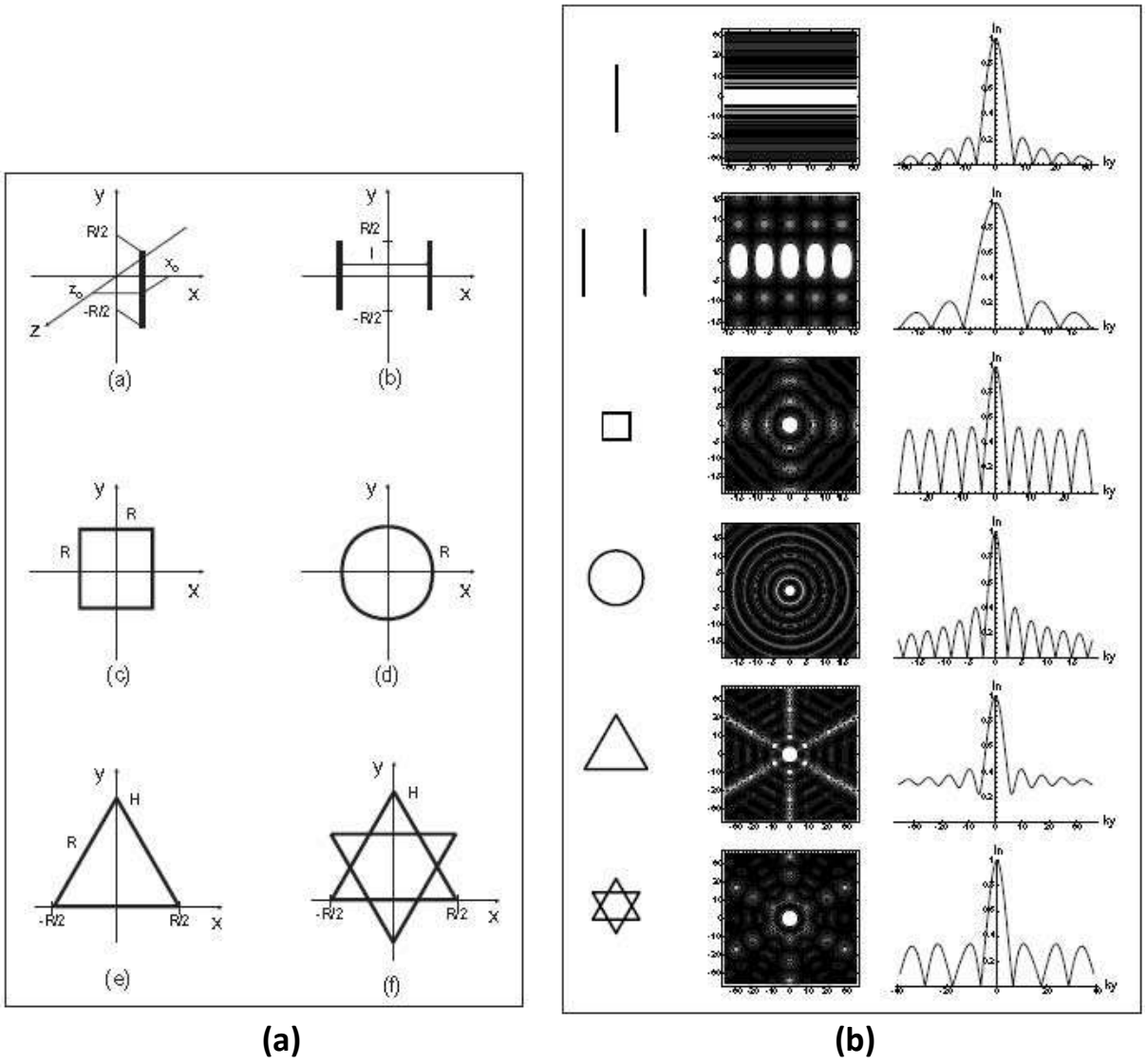

Figure 6. (a) Various 1-dimensional slit geometries (wire geometries) in D-space for which Fourier Transform representations in R-space have been calculated. (b) Comparison plots of normalized modulus, I_n, for all six 1-D objects vs. (k_x, k_y) maps in the middle column and vs. a k_y or k_n plot in the right column.

In Figure 6(b), the central column gives a section plot (or contour plot) of $I_n(k)$, a normalized modulus plot as a function of the R-space coordinates k_x and k_y with y being the vertical direction and x being the horizontal direction (see Figure 6(a)) for the corresponding shape on the left. The right hand column provides a cut through this figure along the k_y-coordinates for all shapes. These plots all correspond to the diffraction pattern of the object shape under consideration.

For the single rod (or slit), the k_y-direction in R-space is colinear with the y-direction in D-space and each oscillation in the modulus, I_n, decays in amplitude as one moves from the center of the slit to either end.

Increasing the length of the slit (rod) reduces the size of the undulation intervals, Δk_y, for the bumps in the I_n profile.

For the **two parallel rods (slits)**, displaced from each other by a distance ℓ in the x-direction, a phase-difference of e^{ilk_x} exists between them. This causes the second slit (rod) to **interfere** with the first to produce a dominant oscillation in I_n along the k_x-direction. For any other polyhedral-shaped rod/slit type of object, parallel segments produce R-space oscillations in the orthogonal directions. (Reference 4, pages 253 to 270 plus the chapter appendices provide abundant additional detail on this topic).

For our purpose, here, the important point to engage the reader's attention is that the above results are remarkably like the classical double-slit experiment of Young for photons (or electrons).

"Whereas a single vertical slit gives a uniform intensity on the screen behind the central region of the slit, a double-slit exhibits a typical interference phenomenon on the screen behind and along a line between the two slits" (the x-direction in Figure 6(a)).

Perhaps what is actually happening in the Young double-slit experiment is that the R-space information pattern of the single and double slit case actually interacts with the photons and guides them to their collision sites on the screen.

This would certainly account for Omura's[12a] observation associated with time-separated, single photon events wherein only one photon was present in the apparatus at a time, yet an interference pattern is present!

This postulate could be seriously tested experimentally by anyone with the necessary apparatus because the details of the photon distribution should mathematically conform to both the **spacing**, ℓ, of the two slits plus their length, L, plus other slit shapes, etc.

When one **complicates**/refines the double slit apparatus with two holes to actually see which hole the photon or electron goes through, the particles behave in a single slit fashion[14].

Further, such an experimental apparatus may be a suitable vehicle for investigating the "deltron-coupler effect" on the R-space pattern detection.

D. An R-space Vector Mathematical Description of the "Remote Viewing" Phenomenon

Julian Schwinger[1], along with Feinman and Tomonaga, shared the Nobel Prize for their discovery and mathematical development of quantum electrodynamics (QED). Schwinger had a Ph.D. student, Paul Werbos, who made the very prophetic points[2] that (1) all forms of QED: Copenhagen, Bohmian, Schwinger-type or Werbos-type yield the same kind of predictions and **none of them** can explain the psychoenergetic phenomenon "remote viewing" and (2) he tells us that the various military establishments of the world have spent billions of dollars using QED to try and "see" things very far away and they have completely failed to do so!

The point, here, is that our present formulation of quantum mechanics (QM), great as it is, is totally inadequate to encompass the inclusion of psychoenergetic phenomena into our scientific worldview, thus, it is time to formulate a larger perspective, or reference frame (RF), for viewing nature that **both** accounts for all of the old successful data **and** also provides the possibility of quantitatively accounting for this new psychoenergetic data in a self-consistent way.

In this regard, Karl Pribram's holonomic theory[15] of brain processing appears to be based on a very slight modification of the **Fourier Transform** duality concept between spacetime information patterns and spectral domain information patterns. His experimental data strongly indicates that cortical neurons of the brain act like individual receiving antennae in a large array which converts spacetime information into a diffraction pattern whose mathematical representation is very close to the Fourier Transform of the incoming spacetime information.

This information conversion to the frequency domain appears to be ideal for subsequent brain processing and brain perception. Of course, the brain must also contain an **inverse** Fourier Transform processor so that our consciousness perceives the outer world structures to be just as we currently think we do.

From a pictoral perspective, one can readily illustrate the structural changes associated with repeated Fourier Transformations in a given direction. These are illustrated in Figure 7 where T represents the Fourier Transformation (clockwise change) while T^{-1} represents the inverse Fourier Transformation (a counter-clockwise change).

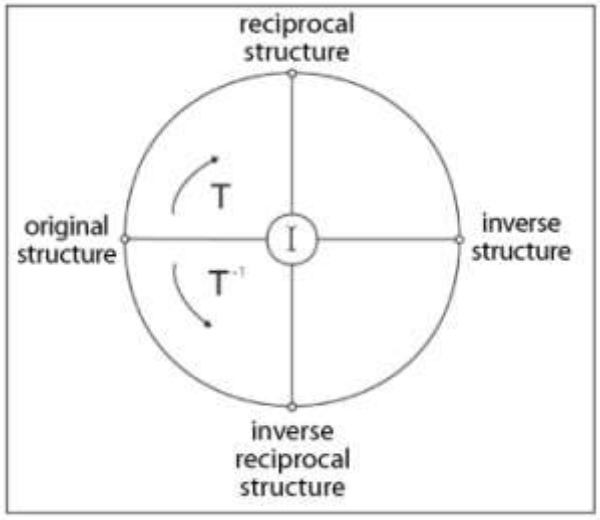

Figure 7. Structural changes associated with repeated Fourier Transformations in a given direction (T = clockwise and T^{-1} = counterclockwise).

From a mathematical perspective, the transformation pair T,T^{-1} for the one-dimensional case can be simply written as

$$T: F(k) = \frac{1}{(2\pi)^{1/2}} \int_D f(x) e^{i2\pi x \cdot k} dx, \qquad (5a)$$

$$T^{-1}: f(x) = \frac{1}{(2\pi)^{1/2}} \int_R F(k) e^{-i2\pi x \cdot k} dk\,. \qquad (5b)$$

The transformation, T, involves the use of the phase operator exp($i2\pi xk$), while the inverse transformation requires using the reverse phase operator exp(-$i2\pi xk$). One is a clockwise rotation while the other is a counter-clockwise rotation. One clockwise rotation of a one-dimensional object, f(x), with spatial coordinate x converting it to a frequency coordinate, (k), representation of the object, F(k), called the reciprocal object which can have mathematically real and imaginary parts. One repeated clockwise transformation, $\tilde{I}$, represents the operation of inversion ($T^2 = \tilde{I}$ and with i^2 = -1) . Four such rotations represents the operation of identity (since T^4 = 1 and i^4 = +1).

In our orthodox science QM paradigm, spacetime-only is the reference frame (RF) used but, to do so, simultaneous particle and wave behavior of all things must be assumed. This created a major philosophical problem for the founding fathers of QM that still exists today, almost a century later. In addition, the psychoenergetic science experiments of Chapters 3 to 5 of Reference 5 have unequivocally shown that human consciousness via focused human intention can significantly influence the properties of materials (inorganic and organic plus in vitro and in vivo).

The key step made by the author of Reference 6 to solve this philosophical problem was to propose an expansion of our RF to a coupled **duplex** RF consisting of reciprocal, 4-dimensional subspaces, one of which is spacetime. Returning to Figure 7, this proposal allows the two ends of the single T-transformation to co-exist as in Figure 8 with the RF for particles being direct space (D-space or (x,y,z,t)-space or spacetime) and simultaneously, the RF for the waves being reciprocal space (or R-space, the physical vacuum space or (k_x,k_y,k_z,$1/t$)-space).

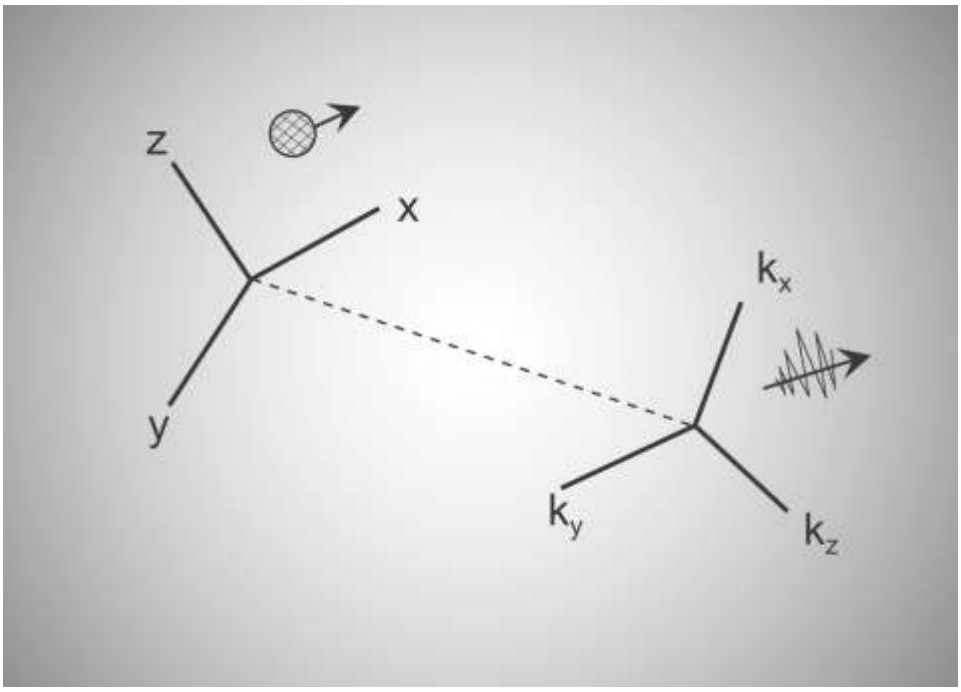

Figure 8. Adoption of the 8-dimensional duplex space as a basis for physical reality would produce a particle and wave simultaneity viewpoint with the RF of the particles being direct space (D-space or x,y,z,t)-space or spacetime). The RF for the waves is labeled reciprocal space (or R-space) or (k_x,k_y,k_z,k_t)-space.

The unique advantage of such a relationship is that, with the addition of a "deltron" coupler[5], a physical property in D-space has a **conjugate** property in R-space given thermodynamically by a deltron-modulated, Fourier Transform relationship such as illustrated via Figure 9[5,6,16].

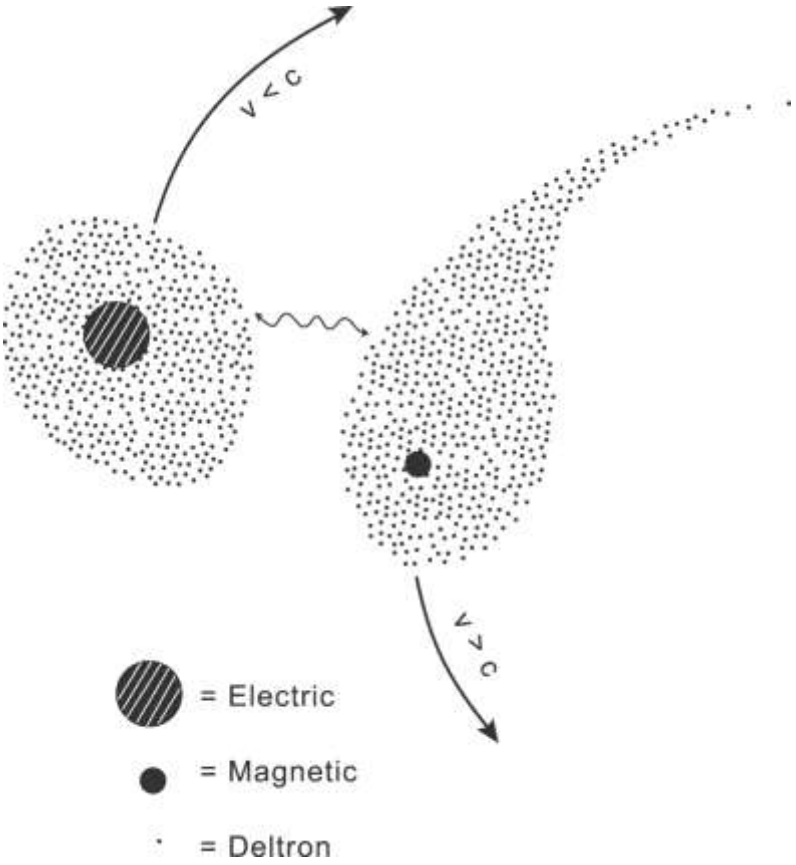

Figure 9. A higher dimensional level substance, labeled deltrons, falling outside the constraints of relativity theory and able to move at velocities v≲c, acts as a coupling agent between the electric monopole types of substances and the magnetic monopole types of substances to produce both electromagnetic (EM) and magnetoelectric (ME) types of mediator fields exhibiting a special type of "mirror principle" relationship between them.

When the deltron coupler concentration is shrunk to zero, these two subspaces are decoupled and we are left with the classical physics picture of a spacetime-only RF; however, when the deltron coupler grows in magnitude, then the QM physics behavior begins to present itself to our world and one can begin to appreciate the importance of human consciousness manifestations in natural phenomena.

The addition of the deltron coupler to our physics concepts increases the magnitude of human-human connectivity as well as human-device connectivity[5-7]. In fact, we can now begin to see how non-local phenomena are operational in spacetime (D-space) via its connectedness with all of R-space and vice versa. It also explains the robust experimental data of References 5,6 and 7. This can now be illustrated via the psychoenergetic phenomenon of **remote viewing**.

Remote Viewing by a Human at Spatial Coordinate (0,0,0,t) and a Physical Object at Coordinates (x,y,z,t)

It is well known that any 3-dimensionally-shaped object, f(x,y,z,t) can be fully described by a 3-dimensional Fourier Transform, $F(k_x,k_y,k_z,k_t)$. Given by

$$F_R(k_x,k_y,k_z) = \frac{1}{(2\pi)^{3/2}}\int_D f(x,y,z)e^{i2\pi s\cdot k}ds \qquad (2a)$$

where s represents (x,y,z) as the D-space coordinates. $F_R(\underline{k})$ is the **conjugate** R-space object description at the distant (x,y,z) location. The modulus, $\tilde{I}_R$, of this Fourier Transform at this remote location is given by

$$\tilde{I}_R = (F_R F_R^*)^{1/2} \qquad (2b)$$

where F_R^* is the complex conjugate of F_R (which is found by replacing all $i = \sqrt{-1}$, the imaginary quantity symbol, by $-i$). This operation converts $\tilde{I}_R$ to a mathematically real quantity with a total value, Q_R, given by

$$Q_R = \int_R \tilde{I}_R(\underline{k})\underline{dk} \qquad (2c)$$

where $\underline{k}$ ranges over the entire frequency domain, (k_x,k_y,k_z) of R-space.

The operational psychoenergetic process of remote-viewing by a person at D-space location (0,0,0) requires the following steps:

(1) Calling the remote R-space location, R_1, and the local observer's R-space location, R_0, one must first translate $F_{R_1}(k_x,k_y,k_z)$ to $F_{R_0}(k_x,k_y,k_z)$, which is mathematically given by

$$F_{R_0}(k_x,k_y,k_z) = \exp(ix+jy+lz)\, F_{R_1}(k_x,k_y,k_z) \qquad (3a)$$

(2) If one also wishes to view the distant object from different angles, an(x,y) rotation by angle θ, say, then $F_{R_0}(k_x,k_y,k_z)$ becomes $F_{R_0}(k'_x,k'_y,k_z)$ where

$$k'_x = k_x cos\theta + k_y sin\theta$$

and (3b)

$$k'_y = k_x sin\theta + k_y cos\theta$$

(3) Finally, $F_{R_0}(k'_x,k'_y,k_z)$ must be transformed back to the D-space representation via using the inverse Fourier Transform (T^{-1}) as in

$$f(0,0,0) = \frac{1}{(2\pi)^{3/2}}\int_R F_{R_0}(k'_x,k'_y,k_z)e^{-i2\pi s\cdot k}dk \qquad (4)$$

(4) Any time-change considerations are dealt with in the same fashion via replacing s with t.

The foregoing steps, 1 to 4, provide a mathematical sequencing for the transformation of the non-local D-space object, f(x,y,z,t), to the viewer's conscious mind in the form of f(0,0,0,t). The actual **inner** human

work to do this occurs at the human unconscious mind or R-space level. It is assumed that, with sufficient training and practice, most (if not all) humans are eventually able to do this as abundant experimental data shows. Further, from a QM-perspective, if the founding fathers had **first** transformed our spacetime-only RF to this particular duplex RF, QM development would have been greatly enriched and enhanced!

E. Material Property Oscillations and Their Coupled Behavior

In Reference 4, Chapter 6, pages 172 to 205 and time period ~May, 1999, in a laboratory near Minneapolis, it was observed that, in an IHD-conditioned space to what we think was the SU(2) Gauge symmetry state level, material properties like air and water, temperature and water pH begin to oscillate in the sub-Hertz range (~10^{-1} to 10^{-6} Hertz). Moreover, the frequencies of all three measurements are identical (the Fourier Transforms absolutely nest, one with the others). Whereas, in our normal U(1) Gauge symmetry state, such an oscillatory behavior never happens. In addition, it appears that the whole room and everything in it oscillates in this way. Figure 10a illustrates how the air temperature-oscillations throughout the room nest while Figure 10b illustrates how both the water temperature-oscillations and the pH-oscillations nest with each other.

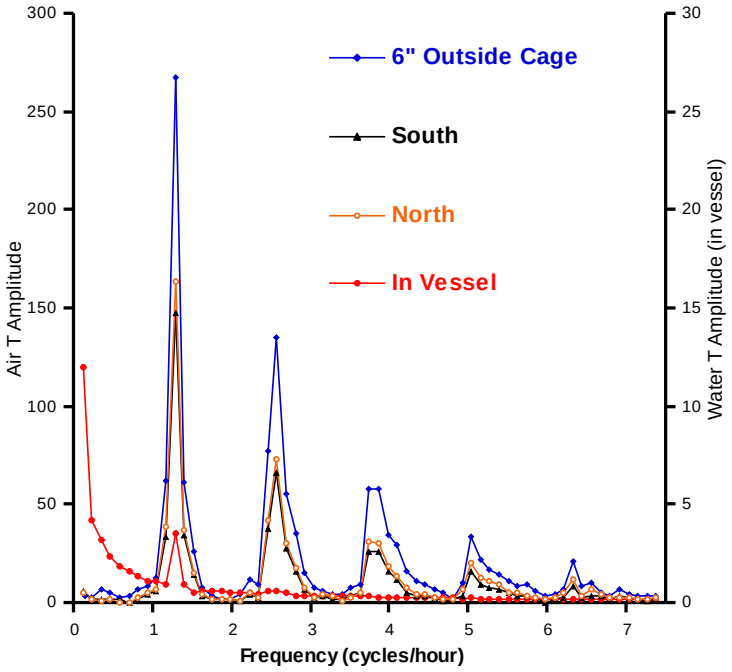

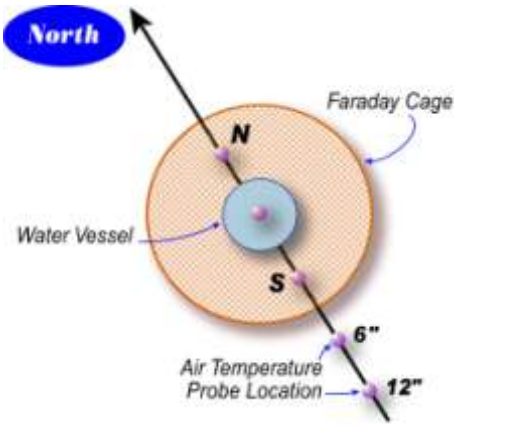

Schematic illustration of air temperature probe locations relative to a centrally located water vessel in an electrically grounded Faraday cage.

Figure 10a. Fourier transformed amplitude spectra data for 9-17.5 hour interval of Figure 10b. The fundamental period is 46.5 min. and five harmonics are observed.

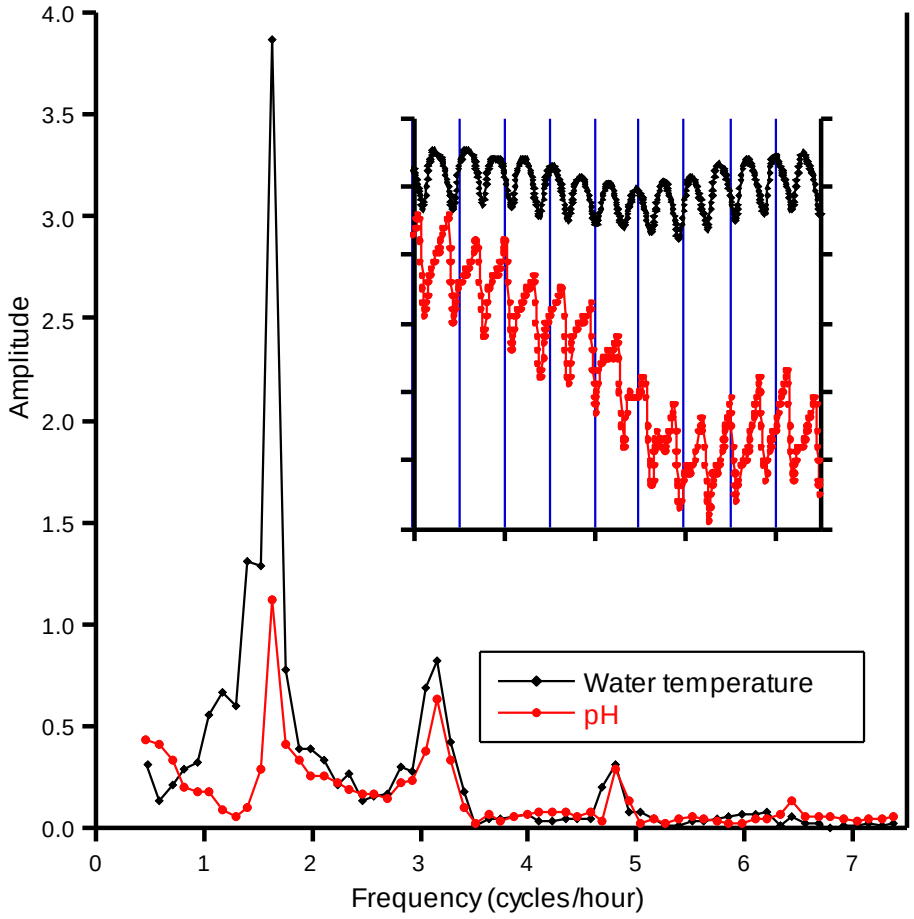

Figure 10b. Fourier Transform comparison of both water T-oscillation and pH-oscillation data in the water vessel on 5/10/99. Real-time oscillation data shown in inset. The fundamental period is 36.6 min. and three harmonics can be easily discerned.

In addition, in Reference 4, pages 202 to 204, when a 6" long natural crystal was placed in the center of the Figure 10a Faraday cage with its c-axis pointing in the vertical direction, the air temperature wave train oscillations located some distance away looked as Figure 11a while, when the orientation of the crystal was shifted to the horizontal orientation at that location, this group of air temperature wave train oscillations immediately inverted its overall shape as in Figure 11b.

(a)

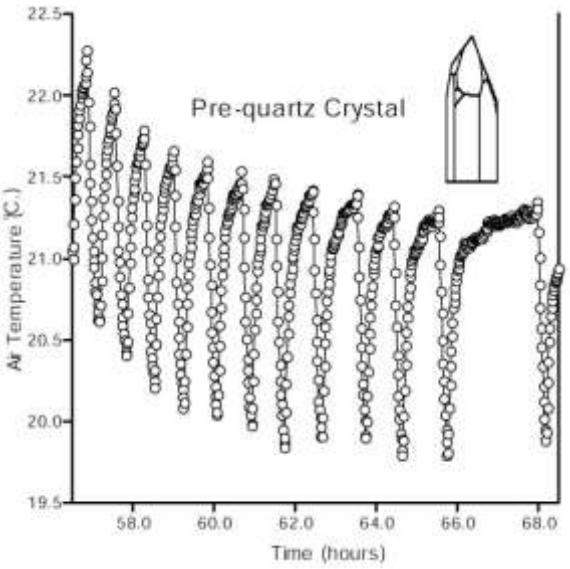

(b)

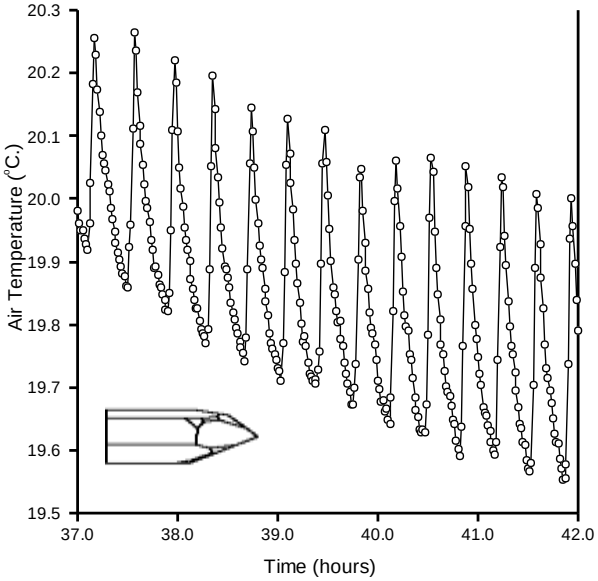

Figure 11a & b. Comparison of air, T-oscillation amplitude, frequency and waveform between the pre-quartz crystal condition and the condition immediately after changing the orientation of the quartz crystal to the c-axis horizontal position.

Clearly, there appears to be some weird material property behavior occurring in IHD-conditioned spaces. Starting in May of 2012 in an IHD-conditioned laboratory located in Payson, Arizona, we discovered a new macroscopic entanglement phenomenon when measuring both pH and air temperature simultaneously in a ~5 foot cubic box with mu-metal walls. These mu-metal walls have a very high magnetic permeability which diverts magnetic flux lines **into** the metal walls so as to significantly lower the total magnetic field intensity in the interior of the box. The two independent

measurement apparati are shown in Figure 12. One measurement system involved a laptop attached via USB cable to a digital thermometer[17]. The other measurement system used its own laptop connected to a pH measurement device via a PCMCIA card (Sensorlink). In the Figure 12 set-up, the two measurement systems are independent but are powered through the same electrical outlets located outside the box.

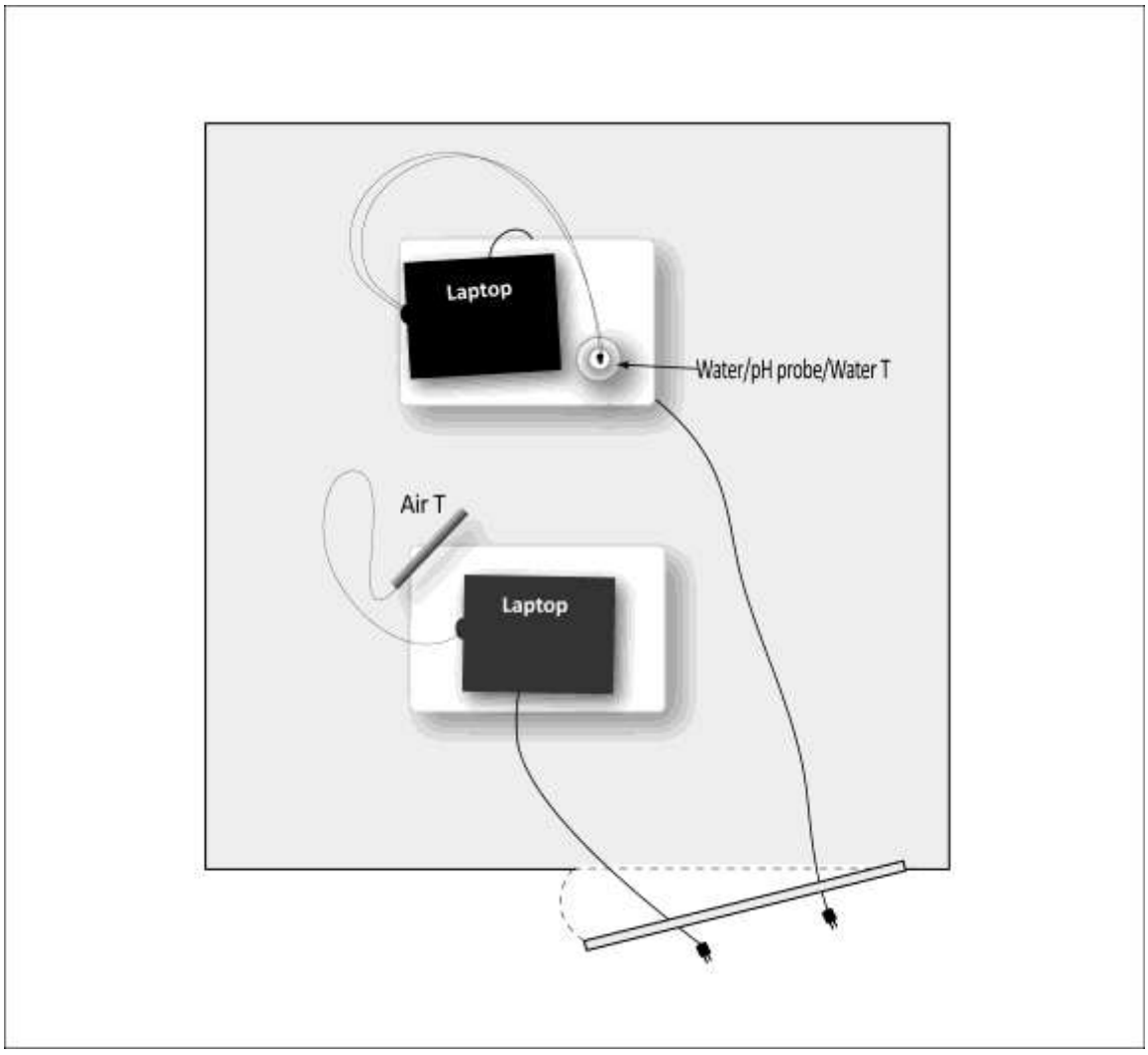

Figure 12. Schematic illustration of Mu-Box experimental set-up.

The air temperature oscillations of interest in this experiment are superimposed on the diurnal air temperature variation which can exhibit high amplitudes since there was no air-conditioning or heating involved. In performing an analysis of oscillation periodicity, we generally de-trended the data to remove the diurnal variation by using a one-hour moving average which yields both 43 and an 86-minute periodicities in the raw data as illustrated in Figure 13.

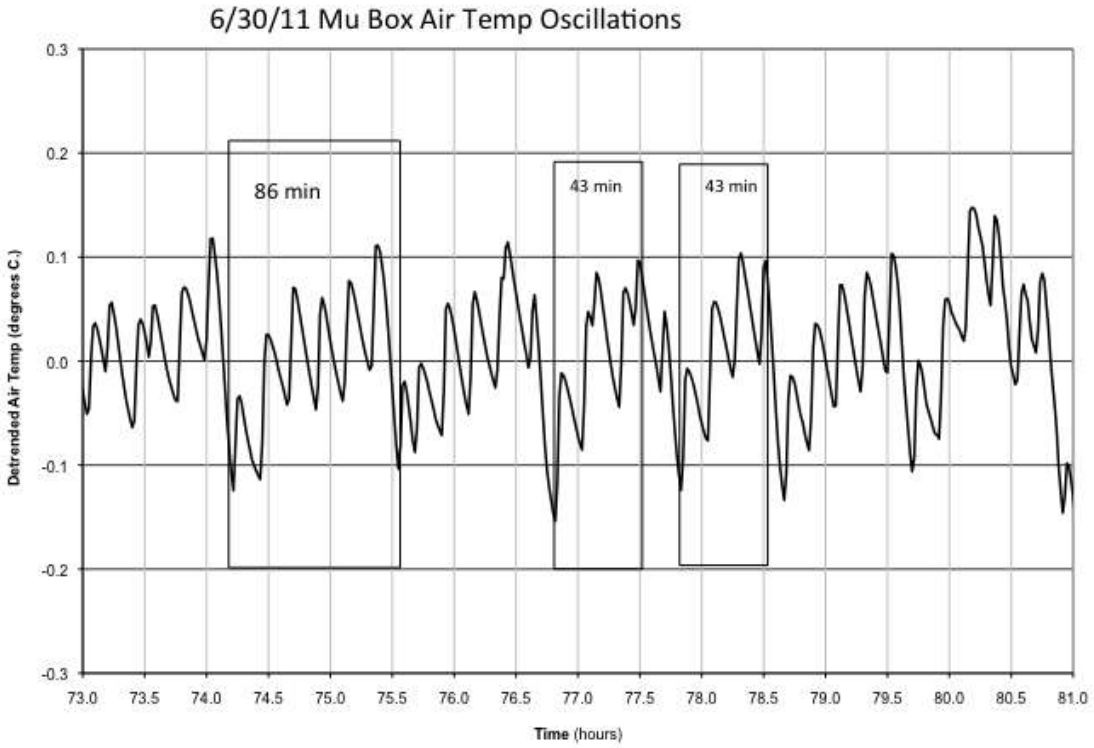

Figure 13. De-trended temperature vs. time.

A Fourier Transformation of this Figure 13 was utilized to provide a more complete picture. This analysis was for a time interval of 6 days using a sample interval of one minute (8640 data points) with the pH-measurement system simultaneously running.

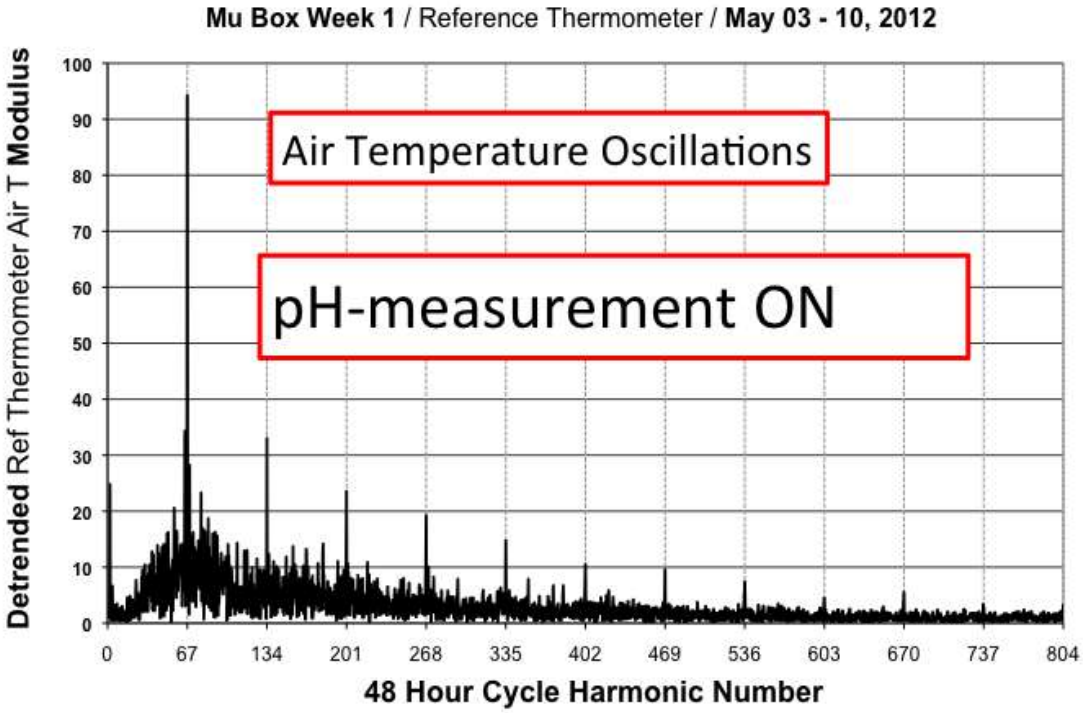

Figure 14a. Modulus vs. 48-hour cycle harmonic number.

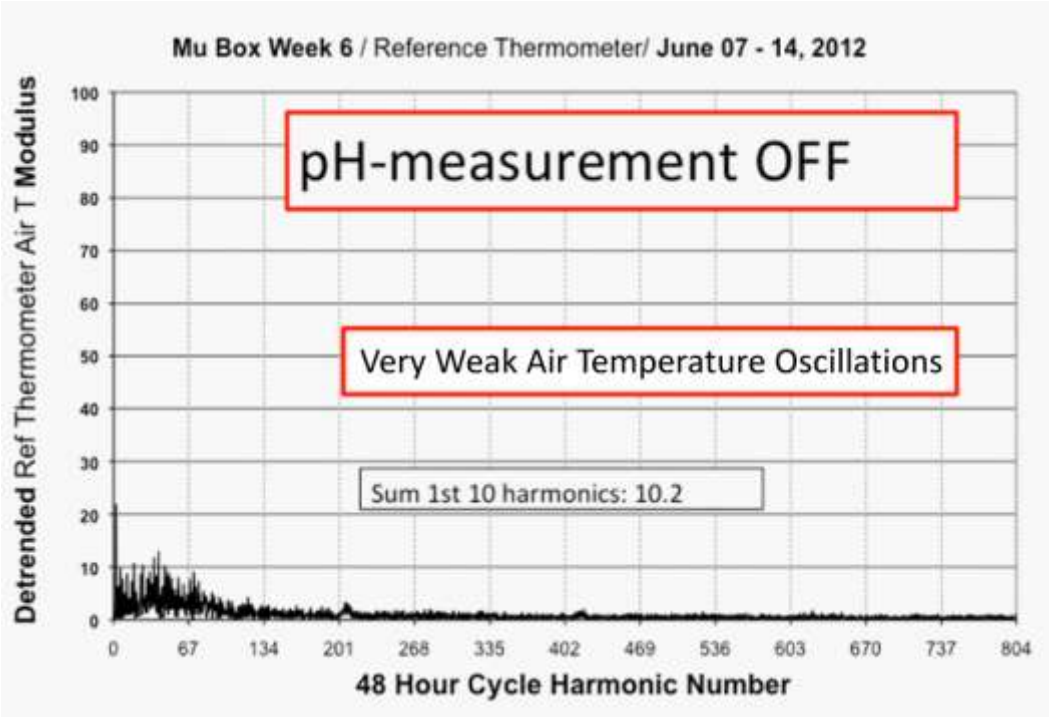

Figure 14b. Modulus vs. 48-hour cycle harmonic number.

Figure 14a shows that this air temperature data has a period that is the 67th harmonic of the 48 hour

cycle. This period is about 43 minute (2880 minutes in 2/67 days). There are also numerous harmonics of this fundamental frequency (0.00038773 Hz). Note that the first 10 harmonics are particularly strong.

An important discovery was noted when we just turned off the pH measurement system for a period of time (see Figure 14b). Suddenly, the de-trended air temperature modulus greatly decreased in amplitude! Merely pressing an off-button on the pH-software's screen interface window accomplished this feat.

To quantify the air-oscillations magnitude, we summed the modulus values for the first ten harmonics shown in Figure 14a. for each week of a long pH-on/pH-off experiment, these modulus sums were recorded both for the time periods the pH was also being recorded and when it was not being recorded. Figure 15a shows the initial results while Figure 15b shows 5 on/off cycles of data gathered over a 10 month experiment.

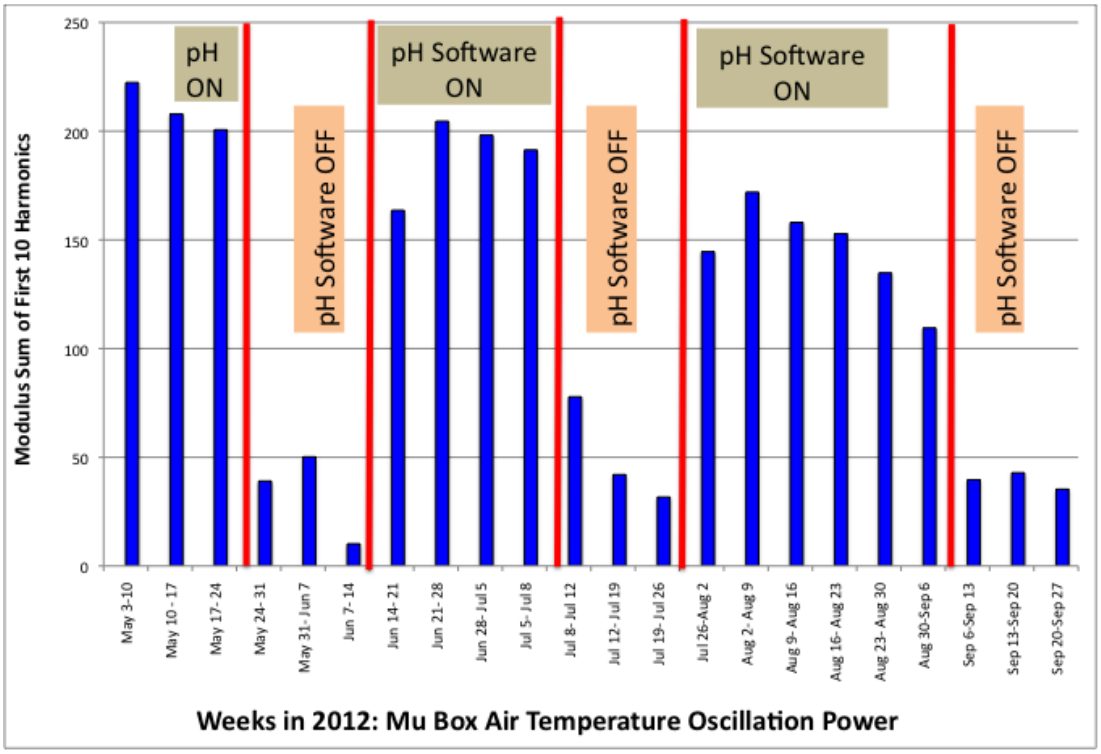

Figure 15a. Modulus sums (power) for each week of the experiment.

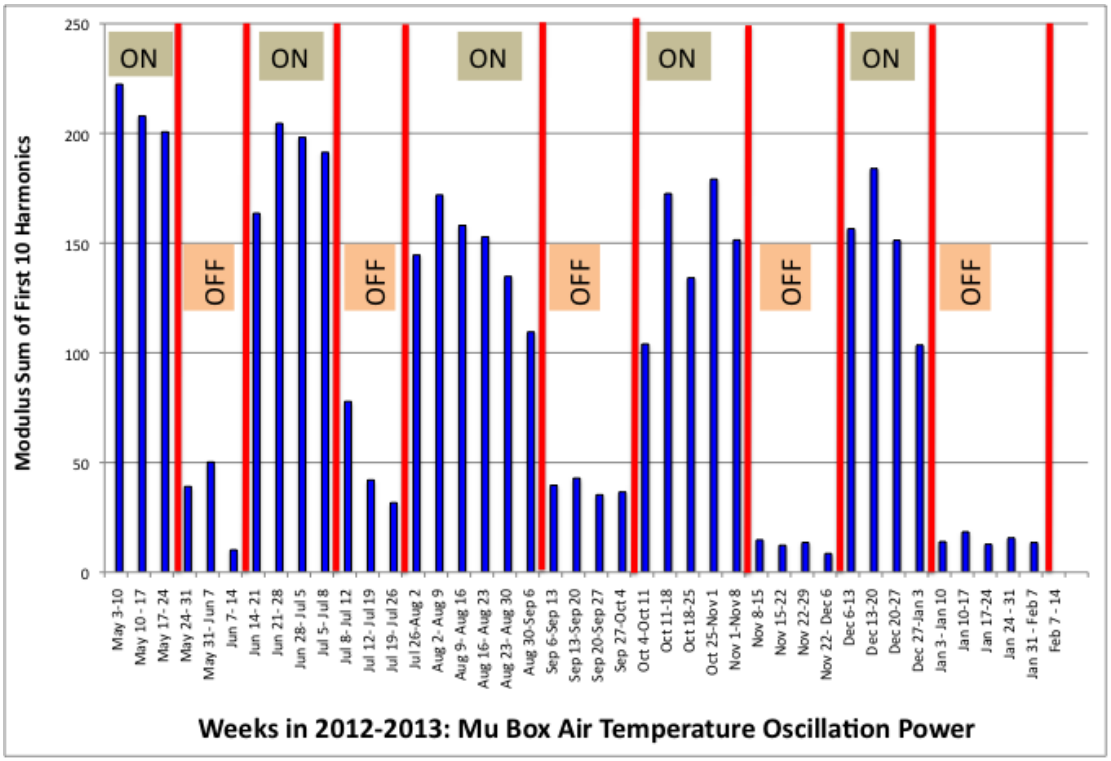

Figure 15b. Modulus sums (power) for each week of the experiment over 10 months and 5 on/off cycles.

One can speculate on the many possible factors influencing the data behavior demonstrated by Figures 15a and 15b. However, this would greatly extend the purpose of adding this topic example to White Paper XXXIX. Thus, we will restrict our attention to the unquestionable entanglement of the pH and temperature measurement systems and propose that this is yet another example of vector behavior of a larger system to be seriously looked at from the perspective of Figures 4 and 5. We presume that Figures 15a and 15b, respectively, refer to the pH-vector being “on” in the system vs “off” in the system.

References

1. J. Schwinger, Particles and Sources (Gordon and Breach, Science Publishers, New York, NY, 1969).
2. P. Werbos, “What do neural nets and quantum theory tell us about mind and reality” in No Matter, Never Mind, eds. K. Yasue, M. Jiba and T.D. Senta (John Benjamins Publishing Co, Philadelphia, PA, 2001).

3. W.A. Harrison, Applied Quantum Mechanics (World Scientific, Singapore, 2000).
4. W.A. Tiller, W.E. Dibble Jr. and M.J. Kohane, Conscious Acts of Creation: The Emergence of a New Physics (Pavior Publishing, Walnut Creek, CA, 2001).
5. W.A. Tiller, Psychoenergetic Science: A Second Copernican-Scale Revolution (Pavior Publishing, Walnut Creek, CA, 2007).
6. W.A. Tiller, Science and Human Transformation: Energies, Intentionality and Consciousness (Pavior Publishing, Walnut Creek, CA, 1997).
7. R.M. Eisberg, Fundamentals of Modern Physics (John Wiley and Sons, Inc, New York, NY, 1961).
8. R.V. Churchill, Introduction to Complex Variables and Applications (McGraw-Hill Book Company, Inc, 1948).
9. W.A. Tiller, "What does the Dirac energy sea mean and why has today's orthodox physics neglected it?", online document, www.tiller.org, White Paper #VI.
10. W.A. Tiller, "Why CAM and orthodox medicine have some very different science foundations", online document, www.tiller.org, White paper #III.
11. M. Enserink, "Can the Placebo be the Cure?", Science, 284, 238-240, 1999.
12. (a) W. Omura, Evolutionary Consciousness (to be published, 2015;
    (b) R. Feinman, L. Leighton and M. Sands, The Feinman Lectures on Physics, Vol 2 (Reading MA; Addison-Wesley, 1981) p 1.
13. W.A. Tiller, online documents. www.tiller.org, White Paper #XXXVII.
14. J. Gribbin, In Search of Schroedinger's Cat (Bantam Books, Inc, New York, NY, 1984) p 171.
15. K. Pribram, Brain and Perception, Holonomy and Structure in Figural Processing (Lawrence Erlbaum Associates, Hillsdale, NJ, 1991).
16. W.A. Tiller, W.E. Dibble, Jr. and J.G. Fandel, Some Science Adventures with Real Magic (Pavior Publishing, Walnut Creek, CA, 2003).
17. USB Reference Thermometer Model #USB-REF from Thermoworks, www.thermoworks.com.

Appendix I, Relevant Mathematics for the Placebo Effect

Here, we use Figure 4 as the most general example of a D-space medical interactive relationship and use it as a pedagogical vehicle for generating the R-space equilibrium counterpart for such a system event.

With $\underline{r}$ representing the D-space general spatial coordinate and $\underline{k}$ representing the R-space general spatial wave number, the Fourier Transform pair relationship for a D-space shape of the form $f(\underline{r})$ is given by

$$F(k) = \frac{1}{(2\pi)^{3/2}} \int_{-\infty}^{\infty} f(\underline{r})\, e^{i\underline{r}\bullet\underline{k}} d\underline{r}\,, \qquad \text{(1-1a)}$$

and

$$f(\underline{r}) = \frac{1}{(2\pi)^{3/2}} \int_{-\infty}^{\infty} F(\underline{k})\, e^{-i\underline{r}\bullet\underline{k}} d\underline{k}\,. \qquad \text{(1-1b)}$$

With a deltron activation function of $C_\delta(\underline{r})C_\delta'(\underline{k})$, the deltron-empowered Fourier Transform pair relationship for a D-space subsystem in the overall system is given by

$$G(\underline{k}) = F(\underline{k})C_\delta'(\underline{k}) = \frac{1}{(2\pi)^{3/2}} \int_{-\infty}^{\infty} f(\underline{r})C_\delta(\underline{r})\, e^{i\underline{r}\bullet\underline{k}} d\underline{r} \qquad \text{(1-2a)}$$

and

$$G'(\underline{r}) = f(\underline{r})C_\delta(\underline{r}) = \frac{1}{(2\pi)^{3/2}} \int_{-\infty}^{\infty} F(\underline{k})C_\delta'(\underline{k})\, e^{-i\underline{r}\bullet\underline{k}} d\underline{k}\,. \qquad \text{(1-2b)}$$

This is how an **equilibrium** R-space conjugate is formed for a given D-space geometrical shape, G'($\underline{r}$), in the partially coupled state of physical reality when the deltron activation function is separable into the $C_\delta(\underline{r})C_\delta'(\underline{k})$ form.

To obtain the $\alpha_{eff}Q_m$ term in Equation 2 of the main text, we first evaluate the intensity, I($\underline{k}$), and integrate it over all of R-space to obtain Q_m. Then, we take general expansions of $C_\delta(\underline{r})$ and $C_\delta'(\underline{k})$ and make a zeroth order approximation to obtain α_{eff}. Proceeding,

$$I(\underline{k}) = G(\underline{k})G^*(\underline{k}) \qquad \text{(1-3a)}$$

and

$$\alpha_{eff}Q_m = \int_{-\infty}^{\infty} I(\underline{k})d\underline{k}\,. \qquad \text{(1-3b)}$$

Here G*($\underline{k}$) is the complex conjugate of the vector G($\underline{k}$).

Turning now to Figure 5 of the main text, there is only one component to Q_e in equation 1 of the main text but 5 vector components for the R-space counterpart. Setting α_{eff} = the space gauge symmetry component, we now have Q_M being determined by the other four vector contributions defined, with subscripts P, D, C and U to represent, respectively, practitioner, device, client and unseen. Therefore, the system vector, $R_s\exp(i\theta_s)$, is given by the vector sum

$$R_S(\underline{k})e^{i\theta_S(\underline{k})} = R_P(\underline{k})e^{i\theta_P(\underline{k})} + R_D(\underline{k})e^{i\theta_D(\underline{k})} + R_C(\underline{k})e^{i\theta_C(\underline{k})} + R_U(\underline{k})e^{i\theta_U(\underline{k})}. \quad (1\text{-}4)$$

The system intensity, $I_s(\underline{k})$, is given by

$$I_S(\underline{k}) = R_S(\underline{k})e^{i\theta_S(\underline{k})}R_S(\underline{k})e^{-i\theta_S(\underline{k})} = R_S^2(\underline{k}) \quad (1\text{-}5a)$$

$$= \left[R_P^2 + R_D^2 + R_C^2 + R_U^2 \right]$$

$$+2\begin{Bmatrix} R_P R_D \cos(\theta_P - \theta_D) + R_P R_C \cos(\theta_P - \theta_C) + R_P R_U \cos(\theta_P - \theta_U) + \\ R_D R_C \cos(\theta_D - \theta_C) + R_D R_U \cos(\theta_D - \theta_U) + R_C R_U \cos(\theta_C - \theta_U) \end{Bmatrix} \quad (1\text{-}5b)$$

In equation 1-5b, the coordinate, $\underline{k}$, has been left out for simplicity. The important point to note here is that, in the system intensity, which is all that one can expect to measure, we have 6 pairwise terms indicating that each term is connected to each other term and each subsystem has three neighboring interactions. For example, let us let the device be replaced by a placebo so that we can represent $I_S(\underline{k})$ by

$$I_S(k) = A + 2R_D \left\{ R_P \cos(\theta_P - \theta_D) + R_C \cos(\theta_D - \theta_C) + R_U \cos(\theta_D - \theta_U) \right\} \quad (1\text{-}6)$$

where A is determined by subtracting equation (1-6) from (1-5b). Thus, even if R_D has only a nominal value, the bracket that multiplies it can be very large so its activity effect in the system can be appreciable. This is how, in a typical doctor, treatment, placebo, subjects randomized clinical trial, the placebo group can **never** be isolated from the treatment group. Further, the magnitude of the placebo effect depends on the size of the doctor effect, the treatment effect, the subject effect and the unseen effect.

If one is using just one subject (client) with the practitioner using a testing device on the subject and one brings a sequence of food supplements, X, say, into the field of the experiment, a series of new terms will enter $I_S(k)$, one for each of the other R-space subsystems in the overall system. In principle, one can use such a testing procedure to determine beneficial vs. harmful reactions of the R-space aspect of X upon the R-space aspect of the client.